Acta Chemica Scandinavica, 1997: 51: 294–301
Printed in UK – all rights reserved

ACTA
CHEMICA SCANDINAVICA
ISSN 0904–213X

Structure and Thermal Behaviour of Dichlorobis(thiourea)cadmium(II), a Single-Source Precursor for CdS Thin Films

Malle Krunks,[a,c] János Madarász,[a†] Lassi Hiltunen,[a] Risto Mannonen,[b] Enn Mellikov[c] and Lauri Niinistö[a*]

[a]Laboratory of Inorganic and Analytical Chemistry and [b]Laboratory of Concrete Technology, Helsinki University of Technology, FIN-02150 Espoo, Finland, and [c]Institute of Materials Technology, Tallinn Technical University, EE-0026 Tallinn, Estonia

Krunks, M., Madarász, J., Hiltunen, L., Mannonen, R., Mellikov, E. and Niinistö, L., 1997. Structure and Thermal Behaviour of Dichlorobis-(thiourea)cadmium(II), a Single-Source Precursor for CdS Thin Films. – Acta Chem. Scand. 51: 294–301. © Acta Chemica Scandinavica 1997.

The title compound (**1**) crystallizes in the space group $Pmn2_1$ with $a=13.110(3)$, $b=5.813(1)$ and $c=6.482(1)$ Å. Its crystal structure was redetermined from three-dimensional single-crystal data to a final R-value of 0.0221. The Cd^{2+} ion is tetrahedrally coordinated to two sulfur atoms from the tiourea ligand (Cd–S = 2.509 Å) and to two chloride ions at distances 2.545 and 2.518 Å. When heated in air or in an inert atmosphere **1** undergoes a complex degradation process which was studied *in situ* by simultaneous TG/DTA as well as by EGA-FTIR. The gaseous species evolved include NH_3, HCl, H_2NCN, HNCS and CS_2, which upon oxidation yield also HCN, SO_2, COS and CO_2. In the solid residue, NH_4CdCl_3 and CdS were detected by X-ray diffraction. Elemental and XPS analyses also indicated the presence of Cl and N as well as some carbon residue. The results of the thermoanalytical study are not directly applicable to the spray pyrolysis process because of the different experimental conditions, but they nevertheless indicate that it is extremely difficult to prepare impurity-free CdS. The formation of HCN, not detected earlier, should also be taken into account when designing the process parameters and safety measures.

Cadmium sulfide has a wide range of potential applications, e.g. in solar cells, photodetectors and gas sensors. The simple chemical deposition of CdS thin films, either using solution techniques or spray pyrolysis, is the most convenient route to low-cost, large area applications.

The thiourea complex of cadmium(II) chloride has frequently been studied because of its use as a single-source precursor for CdS thin films in the spray pyrolysis process.[1] The 2:1 complex $[Cd(SCN_2H_4)_2Cl_2]$ (**1**) can easily be prepared as a crystalline solid by letting the aqueous solutions of thiourea and $CdCl_2$ react at room temperature.[2] In the structure of **1**, the cadmium ion is tetrahedrally coordinated as revealed by an early crystallographic analysis.[3]

The pyrolytic process in air leading to the formation of CdS is a complex one, and therefore several mechanisms, intermediates and evolved gaseous species have been suggested in the literature.[1,2,4–8] When comparing the stoichiometries of the precursor (**1**) and CdS it is obvious that the evolved species must contain C, N, H and S; a possible scheme for the decomposition involves the release of one thiourea ligand as a first step.[1,5]

The aim of the present investigation was to establish the mechanism of the thermal degradation of $[Cd(SCN_2H_4)_2Cl_2]$ in air by a systematic study and thus obtain a better understanding of the spray pyrolytic process leading to CdS thin films. The precursor, its thermal degradation products and intermediates were characterized by X-ray diffraction techniques, while FTIR was used for *in situ* evolved gas analysis (EGA).

Experimental

Synthesis. Single crystals of **1** were grown by mixing 0.2 mol dm^{-3} solutions of thiourea and $CdCl_2$ in the ratio 2:1 and by letting the resulting solution slowly evaporate at room temperature. The crystal shape was that of an elongated prism.

* To whom correspondence should be addressed.
† Permanent address: Institute of General and Analytical Chemistry, Technical University of Budapest, H-1521 Budapest, Hungary.

X-Ray diffraction. The X-ray powder patterns for the precursor (**1**), and its reaction intermediates and products were recorded by a Philips MPD 1880 diffractometer using Cu*K*α radiation.

Single-crystal measurements on **1** were made with a Syntex $P2_1$ four-circle diffractometer using graphite-monochromatized Mo*K*α radiation. Unit-cell dimensions were determined from single-crystal data by least-squares refinement. Intensity data were corrected for Lorenz and polarization effects as well as for absorption. Temperature factors were refined anisotropically except for the hydrogen atoms, for which isotropic temperature factors were refined with positional parameters at calculated positions. Further details of the data collection and structure determination are given in Table 1.

Thermal and FTIR studies. Thermal behaviour was studied in a Seiko TG/DTA 320 instrument. The sample size was 15–30 mg and the heating rate 10 °C min^{-1}. The measurements were carried out in a dynamic air atmosphere (flow rate 80 ml min^{-1}), but for comparison some experiments were made in pure argon (99.95%).

The evolved gas (EGA) studies were carried out with a Bomem TG/Plus instrument consisting of a DuPont 951 thermobalance coupled to a Bomem MB 102 FTIR analyser. The samples (25–60 mg) were heated in a helium flow of 230 ml min^{-1} up to 100 °C, whereupon an oxygen stream of 20 ml min^{-1} was introduced, and the TG run was continued under oxidizing conditions up to 500 °C. The evolved gases were analyzed with the FTIR spectrometer. The interferograms were collected every 30 s. For comparison, an experiment was carried out in pure helium (99.9995%).

Ex situ FTIR was used to study the reaction intermediates and products. The FTIR spectra were obtained in the 4000–400 cm^{-1} range with a Nicolet Magna IR 750 instrument by the KBr pellet technique.

Elemental and XPS analyses. The composition of the samples was also in some cases checked by elemental analyses (C, H, N, Cl, S) carried out by the Analytical Laboratory of Prof. Dr. H. Malissa and G. Reuter GmbH, Gummersbach, Germany. X-Ray photoelectron spectroscopy measurements were performed with a Kratos Analytical AXIS 165 instrument using monochromatized Al*K*α radiation.

Results and discussion

X-Ray diffraction.

Single-crystal study. The unit-cell data of **1** (cf. Table 1) are in agreement with the published dimensions (a= 13.07, b=5.80 and c=6.48 Å).[3] The crystal structure analysis of the precursor (cf. Tables 1 and 2) corroborates the earlier results by Nardelli *et al.*[3] based on photographically recorded intensities. Because of the higher precision of the diffractometer data the atomic coordinates and interatomic distances listed in Tables 2 and 3 deviate in

Table 1. Summary of crystal data, intensity collection and structure refinement for dichlorobis(thiourea)cadmium(II).

Crystal data	
Formula	$Cd(SCN_2H_4)_2Cl_2$
Mol. wt.	327.50
Crystal system	Orthorhombic
Space group	$Pmn2_1$
a/Å	13.110(3)
b/Å	5.813(1)
c/Å	6.482(1)
V/Å^3	494.0
Z	2
d_{calc}/g cm^{-3}	2.20
Radiation	Mo*K*α (λ=0.710 69 Å)
μ(Mo*K*α)/mm^{-1}	3.12
Crystal form	Elongated prism
Crystal size/mm	0.25 × 0.05 × 0.04
Data collection and structure refinement	
Data collection	θ–2θ
Scan speed/° min^{-1}	2–30
No. of data collected	1706
No. of unique data	815
No. of data $I_{obs} > 2\sigma(I_{obs})$	786
Solution and refinement	SHELXL-93
Absorption correction	Empirical
No. of variables	60
Weighting scheme	$1/\sigma^2(F_o^2) + (0.0303\ P)^2$; $P = [\max(F_o^2,0) + 2F_c^2]/3$
$R = \Sigma\|F_o\| - \|F_c\|/\Sigma\|F_o\|$	0.0211
$R_w = [\Sigma[w(F_o^2 - F_c^2)^2]/\Sigma[w(F_o^2)^2]]^{1/2}$	0.0509
Max. peak in difference map/e$^-$ Å^{-3}	0.94

Table 2. Atomic coordinates with isotropic temperature factors for $[Cd(SCN_2H_4)_2Cl_2]$.

Atom	*x*	*y*	*z*	$100U_{eq}$[a]
Cd	0	0.264 29(4)	−0.001 06(3)	3.1
Cl1	0	0.242 55(15)	0.391 02(19)	3.5
Cl2	0	0.689 75(20)	−0.073 71(29)	4.5
S	−0.172 11(5)	0.119 67(11)	−0.110 11(19)	3.5
N1	−0.357 62(34)	0.270 54(46)	−0.066 96(83)	4.9
H11	−0.404 16(34)	0.373 69(46)	−0.053 31(83)	8.6
H12	−0.374 19(34)	0.127 61(46)	−0.074 18(83)	4.6
N2	−0.239 61(24)	0.552 14(38)	−0.065 08(49)	3.5
H21	−0.287 69(24)	0.651 64(38)	−0.051 45(49)	7.8
H22	−0.177 13(24)	0.596 72(38)	−0.071 11(49)	5.5
C	−0.261 72(22)	0.330 97(47)	−0.076 75(48)	2.7

[a] $U_{eq} = \frac{1}{3}\Sigma_i\Sigma_j U_{ij} a_i^* a_j^* a_i a_j$.

Table 3. Bond distances (in Å) and angles (in °) around Cd in the structure of $Cd(SCN_2H_4)_2Cl_2$.

Cd–Cl1	2.545(1)	C–N1	1.307(5)
Cd–Cl2	2.518(1)	C–N2	1.320(3)
Cd–S	2.509(1)	C–S	1.713(3)
Cl–Cd–Cl2	103.63(5)		
Cl1–Cd–S	105.35(3)		
S–Cd–Cl2	106.05(3)		

some cases significantly from the earlier data. The tetrahedral coordination around cadmium is rather regular, with two equivalent sulfurs at a distance of 2.509 Å and the chloride ions at 2.518 and 2.545 Å. The angles around Cd range from 103.6 to 106.0° (Table 3). The discrete molecules of **1** (Fig. 1) are held together by a network of hydrogen bonds involving the NH_2 groups.

Because of its larger size as compared with zinc, Cd^{2+} often prefers octahedral coordination, and only two other thiourea complexes of cadmium are known with a coordination number of four, both containing an oxygen donor ligand (nitrate or sulfate) in addition to thiourea.[9,10] A similar donor atom environment (2 Cl, 2 S) is found in the bis(imidazoline-2-thione) complex, however,[11] where the Cd–S distances are 2.51 and 2.52 Å while the Cd–Cl distances are 2.45 and 2.51 Å.

Powder XRD. The various phases in intermediate and final solid residues were identified with the aid of reference samples and JCPDS files. The CdS phase displayed the expected hexagonal, (greenockite) structure. Our thin films prepared at 300–400 °C by spray pyrolysis were also hexagonal while the chemically deposited CdS films usually have the cubic (hawleyite) structure.[14] In addition to temperature, the precursor appears to play an important role in phase control as shown by studies on the thermolysis of cadmium bis(alkylthiolate) complexes.[15,16]

Thermal analysis. The thermogravimetric (TG) curves are strikingly similar in both air and argon (Figs. 2 and 3) showing three weight loss maxima (from DTG peaks) at approximately 250, 370 and 660 °C, out of which the last one is split indicating a multi-step process. DTA curves, however, show a different behaviour in oxidative and inert atmospheres. In argon all processes are endo-

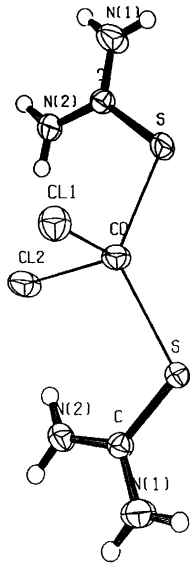

Fig. 1. A perspective view of the $CdCl_2tu_2$ molecule (tu = SCN_2H_4).

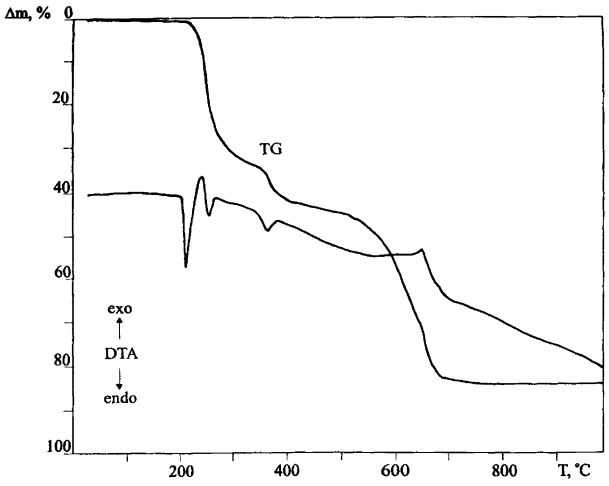

Fig. 2. Simultaneously recorded TG/DTA curves of $CdCl_2tu_2$ in flowing air up to 1000 °C. Sample weight 21.05 mg.

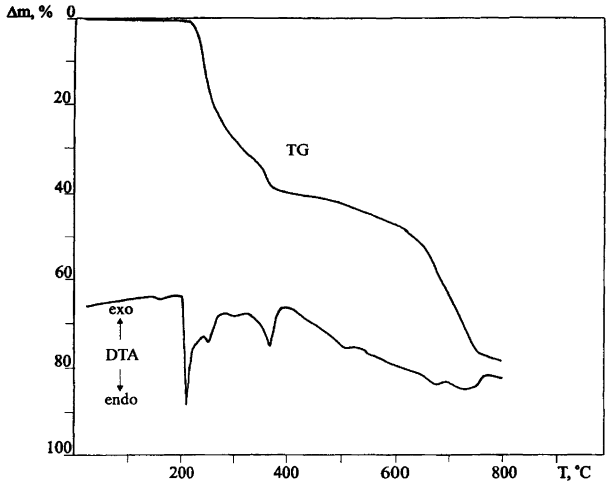

Fig. 3. TG/DTA curves of $CdCl_2tu_2$ in flowing argon up to 800 °C. Sample weight 36.30 mg.

thermic, but in air the first weight loss at 210–240 °C contains both an endothermic and exothermic component, the second process at 330–400 °C is endothermic, whereas the last one at 550–700 °C is exothermic.

Taking into account the X-ray diffraction patterns of the solid residues as well as the IR data, a plausible explanation for the complex TG process can be presented. Because the weight loss by the first DTG minimum at 320 °C (ca. 32%) is clearly higher than that corresponding to the release of only one thiourea ligand (22.7%), the first step must already involve a complete degradation and rearrangement of the cadmium complex. X-Ray diffraction data support this assumption because the formation of NH_4CdCl_3 and hexagonal CdS can be seen in the XRD patterns. Furthermore, IR spectra at 220–300 °C show that thiocyanate is formed through isomerization of thiourea:

$$(NH_2)_2CS \rightarrow NH_4^+ + SCN^-$$

and that no original complex is left (Fig. 4).

NH_4CdCl_3, together with hexagonal CdS, is the dominant crystalline phase at 250 °C both in air and in argon (Fig. 5), but it starts to decompose at 300 °. However, $CdCl_2$ is not detectable in the XRD patterns. At 400 °C the solid residue consists predominantly of CdS. If heating in air is continued, a small amount of $Cd_3O_2Cl_2$ appears above 500 °C, $CdCl_2$ and $CdCN_2$ at 580–640 °C, and finally CdO and $CdCO_3$ above 700 °C. The oxidation of cadmium-containing phases to CdO explains the last exothermic peak in the DTA pattern recorded in air (cf. Fig. 2).

Evolved gas analysis. Evolved gas analysis by FTIR (EGA-FTIR) also shows the extreme complexity of the thermal processes. Figures 6 and 7 summarize the evolution of various gaseous species when the sample is heated in He and an O_2/He mixture, respectively. The identification of the molecules was based on reference spectra or on a characteristic frequency. In Table 4 the gaseous species have been grouped according to four temperature intervals between 210 and 500 °C.

Inert atmosphere. At the first stage (210–320 °C), all gaseous species are decomposition products of thiourea. Neither H_2S nor HCl formation was observed in this temperature range (cf. Fig. 6). The primary reactions are (1) and (2):

$$(NH_2)_2CS(l) \rightarrow HNCS(g) + NH_3(g) \quad (1)$$

$$2(NH_2)_2CS(l) \rightarrow CS_2(g) + H_2NCN(l,g) + 2NH_3(g) \quad (2)$$

Taking into account the composition of the solid phase ($CdS + NH_4CdCl_3$), additional reactions leading to the

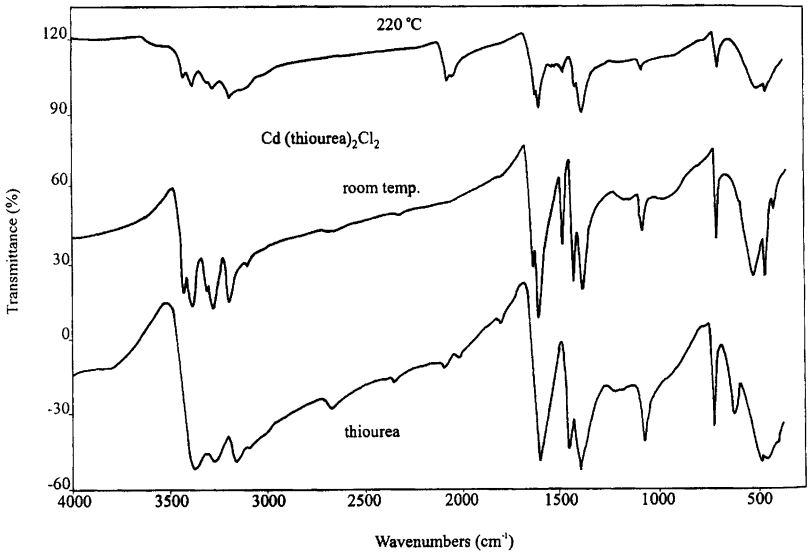

Fig. 4. FTIR spectra recorded at room temperature for thiourea (bottom), $CdCl_2tu_2$ (middle) and for $CdCl_2tu_2$ after its melting and cooling back from 220 °C in Ar (top).

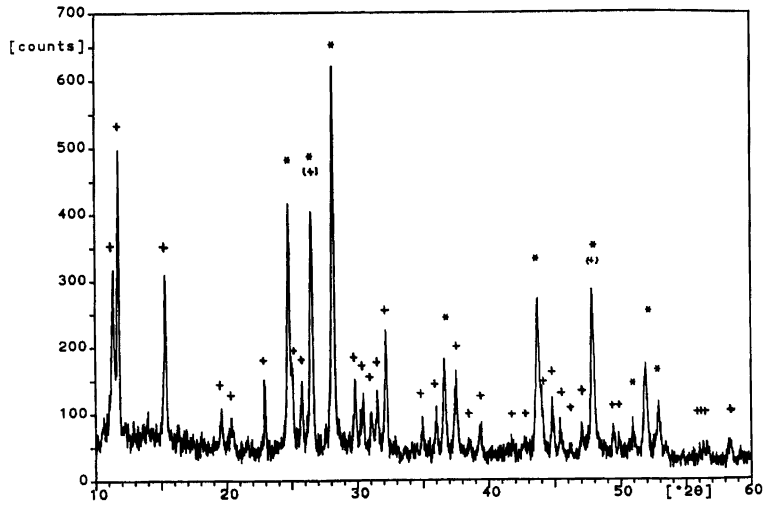

Fig. 5. XRD pattern with phase identification of a sample obtained from $CdCl_2tu_2$ by heating to 270 °C in argon. *, hexagonal CdS; +, NH_4CdCl_3.

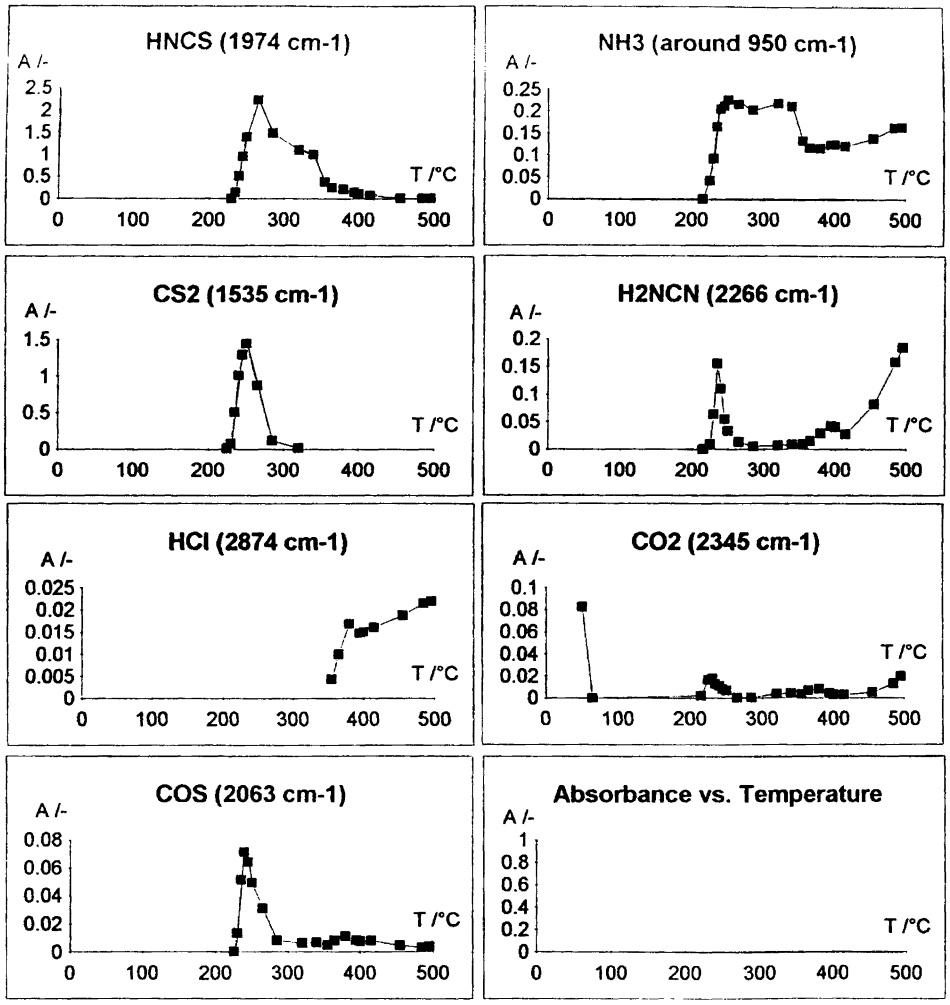

Fig. 6. FTIR absorbance vs. temperature curves of the evolved gases from a $CdCl_2tu_2$ sample in pure He. The axes are identified in the inset in the lower right corner.

Table 4. The observed gaseous species at various stages of the thermolysis in pure He and in a 10% O_2/He mixture.

Stage	Temperature interval/°C	Gaseous species evolved in pure He	Gaseous species evolved in an O_2/He mixture
I	210–320	HNCS, NH_3, CS_2, H_2NCN	HNCS, NH_3, CS_2, H_2NCN, HCN, SO_2, COS, (HCl)
II	320–370	HNCS, NH_3	HNCS, NH_3, HCl
III	370–420	HNCS, NH_3, H_2NCN, HCl	NH_3, H_2NCN, HCl
IV	420–500	NH_3, H_2NCN, HCl	NH_3, H_2NCN, HCl, CO_2

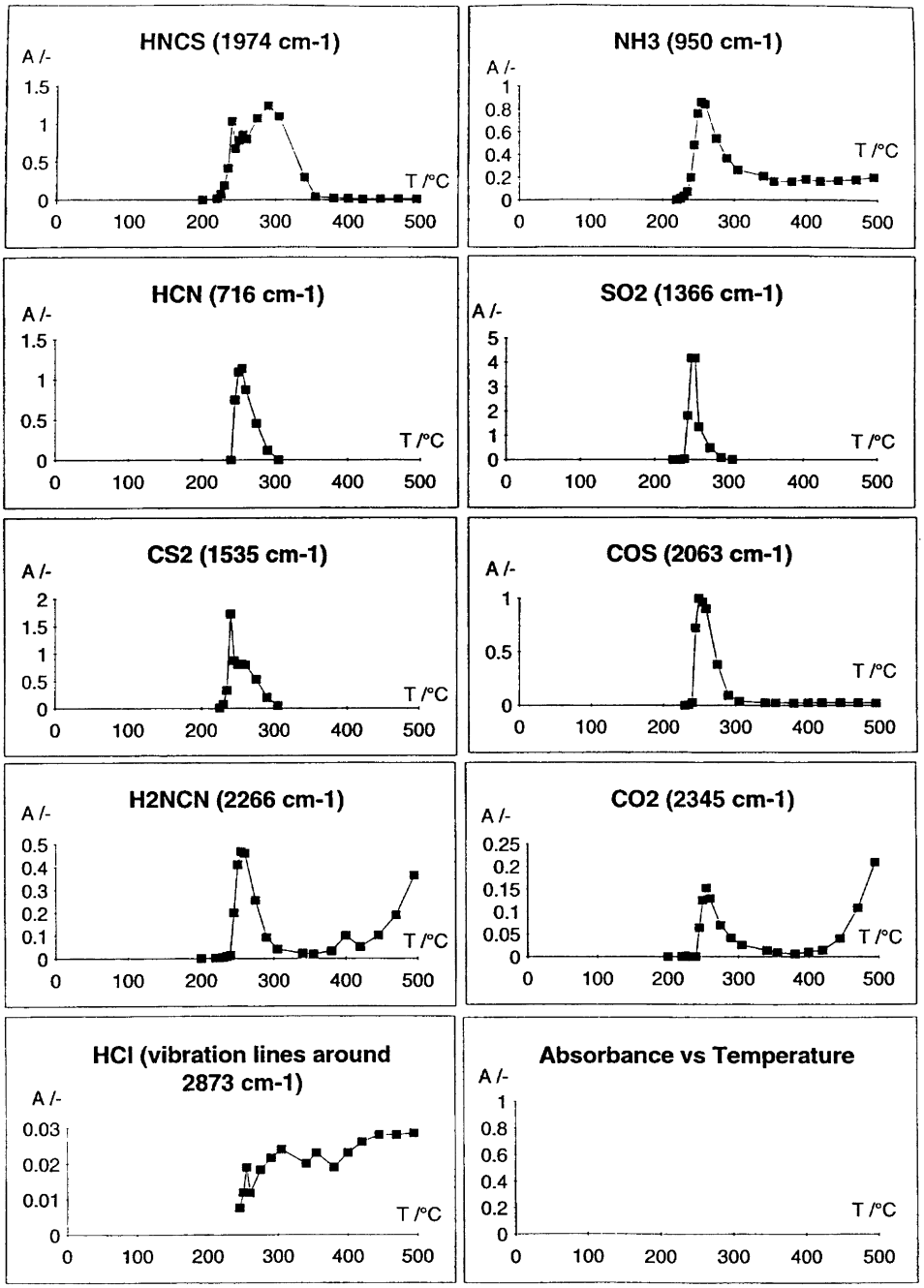

Fig. 7. FTIR absorbance vs. temperature curves of the evolved gases from $CdCl_2tu_2$ in a mixture of He/O_2. The axes are as in Fig. 6.

evolution of H_2NCN and HNCS are (3) and (4):

$$3CdCl_2 + SC(NH_2)_2 + 2NH_3 \rightarrow$$
$$CdS + 2NH_4CdCl_3 + H_2NCN \quad (3)$$

$$3CdCl_2 + CS_2 + 3NH_3 \rightarrow CdS + 2NH_4CdCl_3 + HNCS \quad (4)$$

At these temperatures cyanamide is highly reactive and it may react with other decomposition products or polymerize. The most propable products are guanidinium thiocyanate and melamine. During the second stage (320–370 °C) the evolution of HNCS and NH_3 still continues. The second EGA peak of NH_3 around 350 °C can be attributed to the decomposition of NH_4CdCl_3. This reaction is also the source of increased emission of HCl observed at the end of this temperature range:

$$NH_4CdCl_3 \rightarrow NH_3 + CdCl_2 + HCl \quad (5)$$

Reoccurence of H_2NCN around 400 °C is the most noteworthy feature of third interval (370–420 °C). Its evolution is probably caused by the higher temperature and the presence of free HCl, which facilitate the decomposition of the organic compounds formed earlier. The evolution of cyanamide also continues during the fourth stage, probably because the thermally stable guanidine derivatives such as melamine then degrade.

The amount of released HCl likewise increases with the temperature obviously because cadmium cyanamide is formed (6):

$$CdCl_2 + H_2NCN \rightarrow CdCN_2 + 2HCl \quad (6)$$

Indeed the IR spectrum of the solid residue obtained in an argon atmosphere at 800 °C contained only the vibrations due $CdCN_2$, namely those at 2000–2200 and 650 cm^{-1}.[12]

Oxidizing atmosphere. During the first stage of decomposition (210–320 °C), besides the products mentioned above, several new gaseous oxidation products also occur, such as SO_2, HCN, COS and CO_2. The first three originate from the oxidation of HNCS and CS_2 according to reaction (7) and probably (8):

$$HNCS + O_2 \rightarrow HCN + SO_2 \quad (7)$$

$$CS_2 + 1.5\ O_2 \rightarrow COS + SO_2 \quad (8)$$

These reactions occur suddenly as a mild explosion generating a great deal of heat, observed even in the thermocouple signal as a deviation from linearity. This exothermic heat effect seems to accelerate the other chemical processes as well. The evolution of CO_2 indicates an early partial oxidation of the rearranging organic substances. Also the evolution of HCl already begins at the first stage, which is earlier than in the inert atmosphere.

During the final stages (380–500 °C) the recurrence of cyanamide and CO_2, together with some unidentified vibration bands in the 1400–1660 cm^{-1} region, indicates that the organic part of the condensed phase is decomposing in oxidative ways as well. Probably the oxidation of cadmium cyanamide forming according to reaction (6) also contributes to the CO_2 evolution:

$$CdCN_2 + 1.5O_2 \rightarrow CdO + CO_2 + N_2 \quad (9)$$

The formation of CdO from $CdCN_2$ has been reported in the literature to occur around 400–500 °C.[12] We have found by XRD a small amount of $Cd_3O_2Cl_2$ at 520 °C but found CdO and $CdCO_3$ only above 720 °C. The $CdCO_3$ phase is readily formed by the reaction between the oxide and the evolving carbon dioxide. Also the $Cd_3O_2SO_4$ phase can only be detected in the final residue at higher temperatures (>700 °C). The observed temperatures for the occurrence of CdO and $Cd_3O_2SO_4$ in the CdS preparations are higher than those reported recently,[13] but this may well be due to the different experimental conditions.

Table 5. Results of elemental analyses (in wt. %) of samples prepared by dynamic heating of the precursor to 420 °C.

Atmosphere	C	H	N	S	Cl	Cd[a]
Air	5.24	0.42	9.92	7.04	20.71	56.67
Argon	5.20	0.36	9.94	7.04	20.42	57.04

[a] By difference.

Elemental and XPS analyses. In order to evaluate quantitatively the amount of impurity phases in the CdS residue formed by pyrolysis, two samples were subjected to elemental analysis. The samples were prepared in a thermobalance at 420 °C in both air and argon under identical experimental conditions (instrument, heating rate) as the TG/DTA runs discussed above. The results (Table 5) indicated considerable amounts of C, N and Cl, but amazingly only an insignificant effect of the atmosphere. The chlorine residues are significantly higher than those reported earlier in the thin films prepared by spray pyrolysis at this temperature,[17] and therefore an XPS study of the thin films was undertaken.

XPS data obtained by recording the surface spectra indicate a Cl content of only 3.0 wt.% for a thin film prepared at 420 °C, which is in agreement (2.0%) with the earlier results by chemical analysis.[17] The chlorine content increases when the deposition temperature is lowered, being 6.8 wt.% at 220 °C. Recent Auger data have also revealed localized areas of high chlorine content on the surface of CdS films prepared by spray pyrolysis at lower temperatures.[18] The higher chlorine content found in our bulk samples compared to thin films may be due to fact that the volatile species are trapped in the thermobalance crucible, whereas they are more easily blown away from the open substrate surface during thin-film deposition.

Conclusion

Although $[Cd(SCN_2H_4)_2Cl_2]$ is structurally a simple complex which forms discrete molecules in the solid

state, its pyrolysis is an extremely complicated process leading to several volatile and solid species. The main decomposition product under spray pyrolytic conditions is CdS but it appears not to be possible to produce CdS thin films without significant amounts of chlorine and other impurities. This disadvantage must be taken into account when considering the obvious merits of the precursor, which include its straightforward synthesis and single-source character.

Acknowledgements. A scholarship from the *Viro Säätiö* (Estonia Foundation) to M.K. and support from the Estonian Scientific Foundation (grant no. 1432) and EU contract ERBCIPDCT 930326 are gratefully acknowledged. J. M. acknowledges the scholarship and support from the National Scientific Research Foundation (OTKA, Hungary, grants nos. W-015699 and F-014518). Dr. L.-S. Johansson is thanked for the XPS analyses.

References

1. Krunks, M., Mellikov, E. and Sork, E. *Thin Solid Films 145* (1986) 105.
2. Stoev, M. and Ruseva, S. *Monatsh. Chem. 125* (1994) 599.
3. Nardelli, M., Cavalca, L. and Braibanti, M. *Gazz. Chim. Ital. 87* (1957) 137.
4. Bailey, R. A. and Tangredi, W. J. *J. Inorg. Nucl. Chem. 38* (1976) 2221.
5. Dutault, F. and Lahaye, J. *Bull. Soc. Chim. Fr.* (1979) 145.
6. Ugai, Ya. A., Semenov, V. N., Averbach, E. M. and Shamsheeva, I. L. *Zh. Obshch. Khim. 56* (1986) 1945.
7. Brown, B. J. and Bates, C. W., Jr. *Thin Solid Films 188* (1990) 301.
8. Makurin, Yu. N. and Zhelonkin, N. A. *Neorg. Mater. 30* (1994) 279; *Inorg. Mater. (Engl. Transl.) 30* (1994) 267.
9. Swaminathan, S. and Natarajan, S. *Curr. Sci. 36* (1967) 513.
10. Cavalca, Chiesi Villa, A., Mangia, A. and Palmieri, C. *Inorg. Chim. Acta 4* (1970) 463.
11. Cavalca, L., Domiano, P., Musatti, A. and Sgarabotto, P. *Chem. Commun.* (1968) 1136.
12. Dvoinin, V. I., Skornyakov, L. G., Yatlova, L. E., Degtyarev, M. V. and Kitaev, G. A. *Zh. Prikl. Khim. 55* (1982) 213; *J. Appl. Chem. (Engl. Transl.) 55* (1982) 190.
13. Sebastian, P. J. and Hu, H. *Adv. Mater. Opt. Electr. 4* (1994) 407.
14. Melo, O. de, Hernández, L., Zelaya-Angel, O., Lozada-Morales, R., Becerril, M. and Vasco, E. *Appl. Phys. Lett. 65* (1994) 1278.
15. Osakada, K. and Yamamoto, T. *Inorg. Chem. 30* (1991) 2328.
16. Kräuter, G. and Rees, W. S. Jr. *J. Mater. Chem. 5* (1995) 1265.
17. Krunks, M., Mellikov, E., Sork, E. and Vidrevich, M. *Tallinna Polüt. Inst. Toim. 587* (1984) 49.
18. Pence, S., Bates, C. W. Jr. and Varner, L. *Mater. Lett. 23* (1995) 195.

Received May 7, 1996.